Title

Modeling and Simulations of Methane Heat Exchange Reformer for Fuel Cell Applications

Authors
Keyur S. Patel, Aydin K. Sunol

Affiliations
Department of Chemical Engineering,
University of South Florida,
4202 E. Fowler Avenue,
Tampa,
Florida 33620
USA

In last decade, interest in cleaner energy technologies such as fuel cells has increased significantly, particularly for power generation and automobile applications. Steam reforming of methane, which has significant potential in fuel cell applications, is also industrially important reaction that is employed in production of ammonia, methanol and in Fischer-Tropsch synthesis [1,2]. In conventional tubular reactor for production of methane from hydrogen, the required heat for reaction is provided indirectly by flue gas flowing in annulus. High endothermicity of reforming reaction and limited wall heat transfer coefficient requires considerable energy input requirement in such reactor [3]. For small scale uses the fuel processor has to be compact and at the same time has to have better heat transfer characteristics to increase the hydrogen production. In the heat exchange reformer designed by Haldor-Topsoe, combination of cocurrent and countercurrent flow arrangement between flue gas and process gas is devised to maximize the heat recovery and the hydrogen production. Previous simulation study on methane heat exchange reformer simplified the model by considering each catalyst bed as a well mixed reactor [4]. Since such simplification doesn't represent actual process accurately, we present the improved model without an assumption of the well mixed reactor.

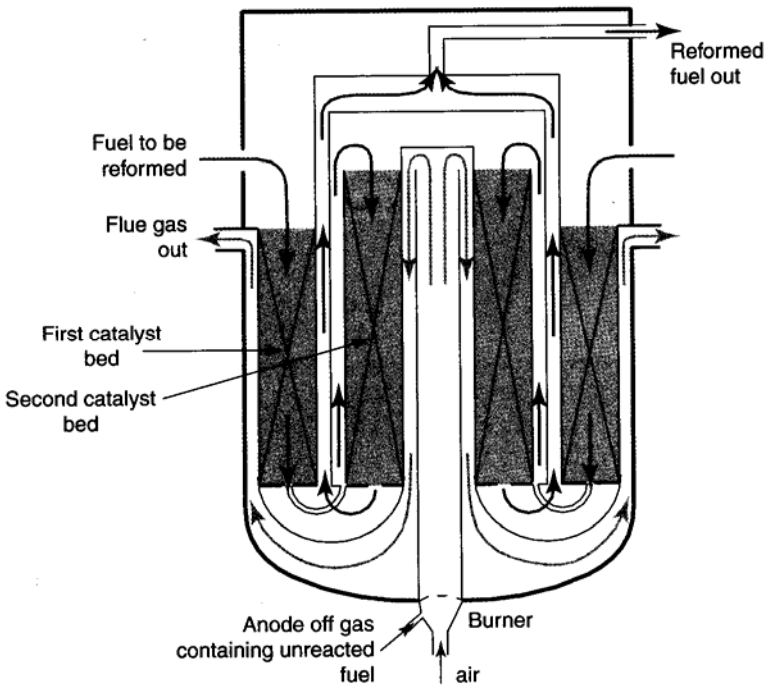

Fig. 1. Schematic diagram of Haldor-Topsoe heat exchange reformer ([5]).

As shown in Fig. 1., the Haldor-Topsoe heat exchange reformer comprises of two catalyst bed. Feed gas flows downwards through first catalyst bed where it is heated by convection from both the flue gas and the reformed product gas, both flowing countercurrent to the feed. After leaving the first catalyst bed, the partially reformed gas is fed to the top of second catalyst bed where it is heated by flue gas and the partially reformed process gas as

shown in Fig. 1. Both catalyst beds are filled with Ni/MgO-Al_2O_3 catalyst where steam reforming of methane takes place. The kinetic information of the reaction is taken from [6]. The temperature and composition dependence of viscosity of the burner gas mixture and the reformer gas mixture is incorporated in the model. Axial diffusion of heat and mass in the reformer and the flue gas is neglected. Pressure inside both the burner, the reformer and is assumed to be constant. Conduction and convection are assumed to be predominant heat transfer mechanism while radiation effect is neglected. Heat loss to surrounding is neglected and both the process gas and the fuel gas are treated as an ideal gas.

The material and energy balance equations result in a set of 20 partial differential equations which are discretized using orthogonal spline collocation on finite elements [7]. The reactor length is divided into 6 intervals with 3 collocation points in each interval. Discretized partial differential equations along with boundary conditions form system of stiff differential algebraic equations which are solved using stiff integrator that utilizes variable order solver based on numerical differentiation formulas. The computations are performed using MATLAB programming environment. Dynamic effects of various operating conditions like steam/methane ratio, inlet gas temperatures and gas inlet velocities are investigated by numerical simulations. From results, reactor performance is analyzed based on methane conversion for above stated operating conditions.

Dynamic and steady state simulations for the base case

Results for only base case simulations are presented and discussed here. Fig. 2(a) and Fig. 2(b) show concentration profiles of the reformer product gas, the burner product gas and the outlet sweep gas vs. time. Profiles indicate that reactor reach steady state in about 600s. The dynamic simulations are followed by the steady state simulations. Temperature profiles obtained from the steady state simulations are shown in Fig. 3(a) and Fig. 3(b). As shown in Fig. 3(a), the flue gas temperature decreases from 1200 K to 1050 K as it passes the second catalyst bed. Further heat recovery is achieved as it flows along the first catalyst bed with the exit temperature reaching 900 K. At the same time, the reformer inlet gas is heated from 400 K to 810 K as it passes along the first catalyst bed. The temperature of product gas coming out from the second catalyst bed reaches 840 K and decreases further to 690 K as it passes along the first catalyst bed. Fig. 3(b) indicates steady state temperature profiles of wall. Here, the first and the fourth wall represent the two side of the second catalyst bed while the second and the third wall represent two side of the first catalyst bed. Steady state concentration profiles are shown in Fig. 3(c) and Fig. 3(d). As shown in Fig. 3(c), the inlet processes gas is partially reformed in first catalyst bed with methane conversion of 28 %. The methane conversion reaches 58 % as on the exit of the second catalyst bed as shown in Fig. 3(d).

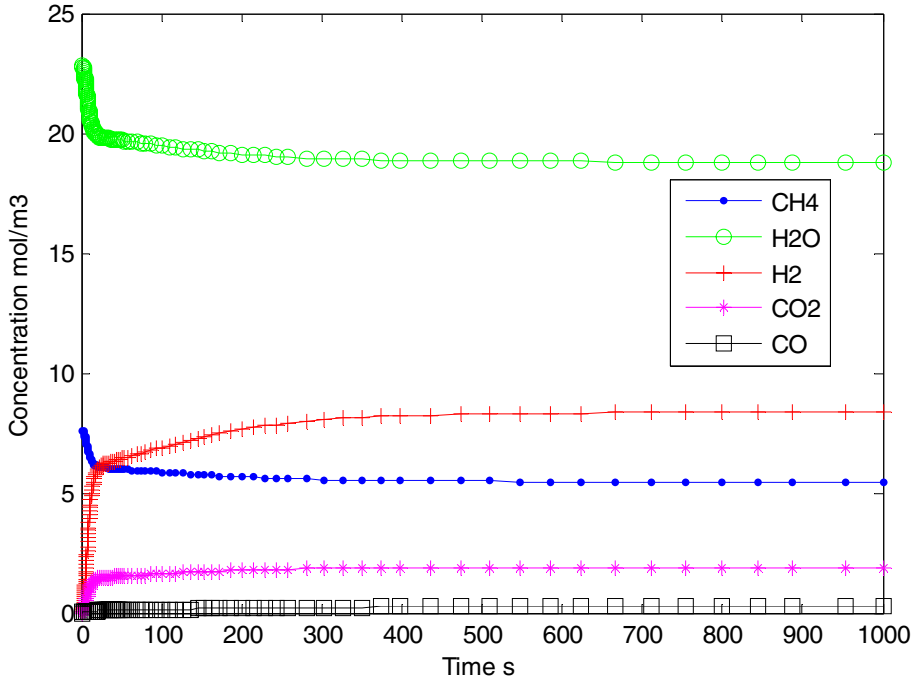
Concentration mol/m3
Time s
CH4
H2O
H2
CO2
CO
0
5
10
15
20
25
0
100
200
300
400
500
600
700
800
900
1000

(a)

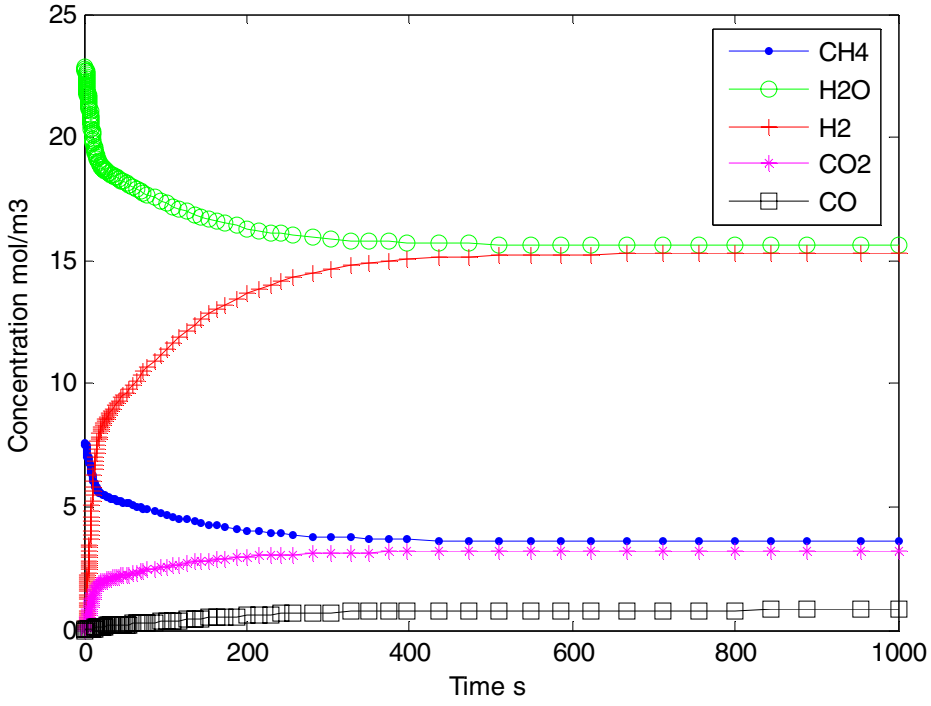
Concentration mol/m3
Time s
CH4
H2O
H2
CO2
CO
0
5
10
15
20
25
0
200
400
600
800
1000

(b)

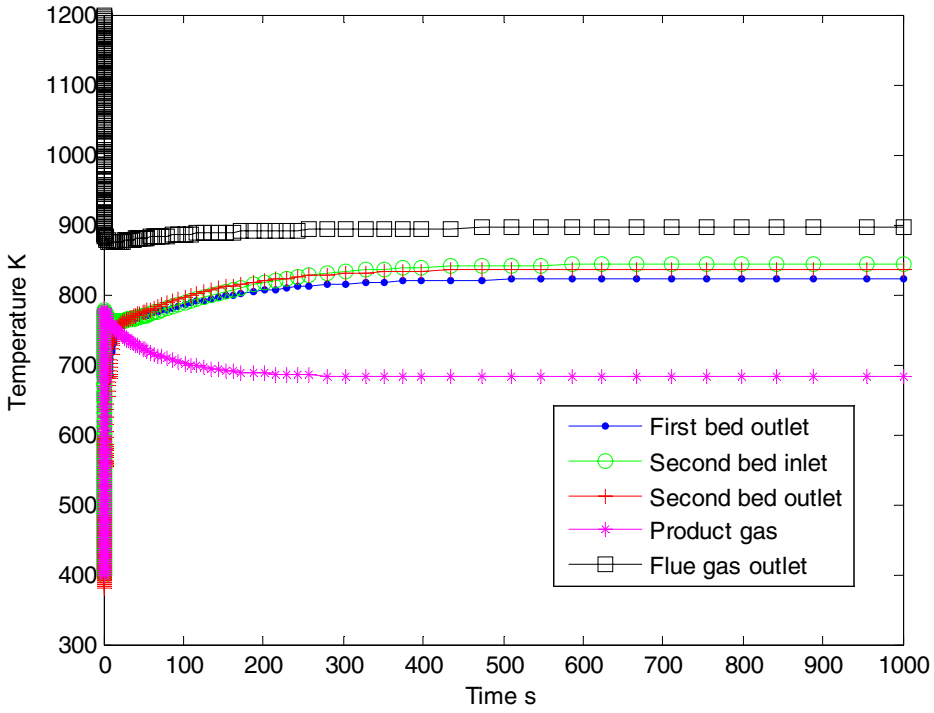

(c)

Fig. 2. Dynamics of (a) reformer product gas composition for the first catalyst bed, (b) reformer product gas composition for the second catalyst bed and (c) flue gas and product gas temperatures.

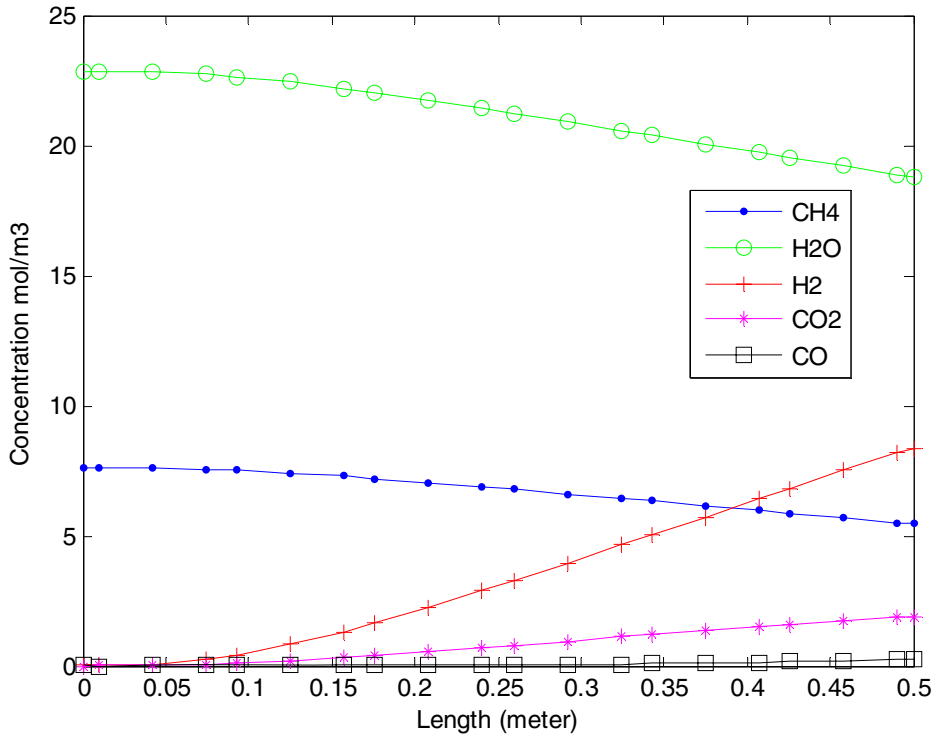
Concentration mol/m3
Length (meter)
CH4
H2O
H2
CO2
CO
0
5
10
15
20
25
0
0.05
0.1
0.15
0.2
0.25
0.3
0.35
0.4
0.45
0.5

(a)

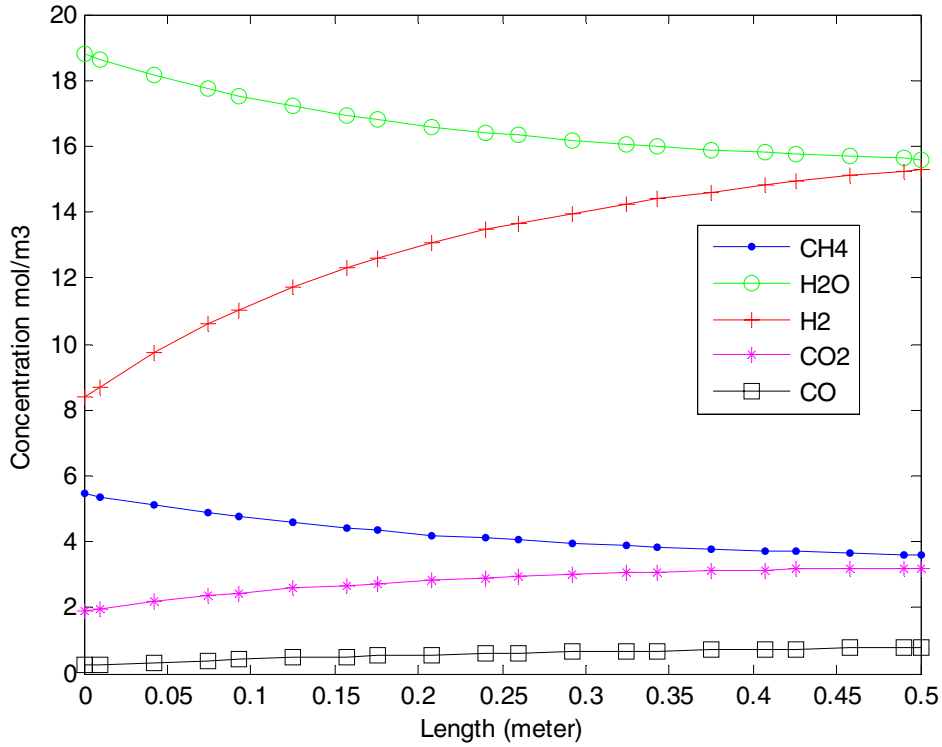
Concentration mol/m3
Length (meter)
CH4
H2O
H2
CO2
CO
0
2
4
6
8
10
12
14
16
18
20
0
0.05
0.1
0.15
0.2
0.25
0.3
0.35
0.4
0.45
0.5

(b)

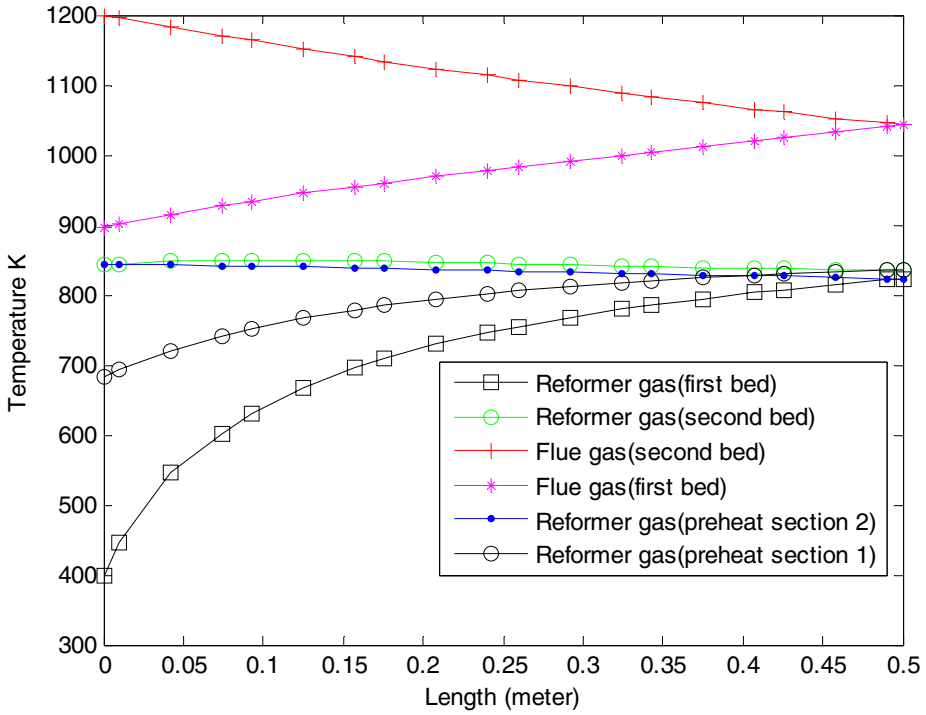

(c)

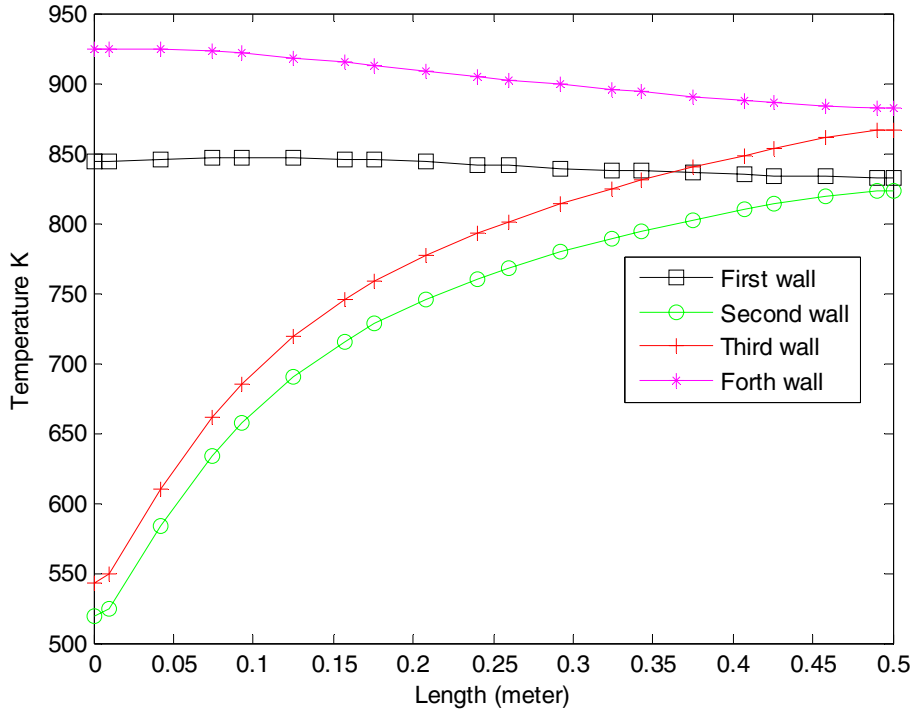

(d)

Fig. 3. Steady state simulations for the base case (a) concentration profiles for the first catalyst bed (b) concentration profiles for the second catalyst bed (c) temperature profiles of flue gas and process gas (d) temperature profiles of wall.

As stated earlier, dynamic effects of change in various operating conditions like steam/methane ratio, inlet gas temperatures and gas inlet velocities are investigated by numerical simulations successfully. Such information is very important for devise the suitable control strategy for the reactor. Results are also helpful to analyze the performance of the reactor based on the methane conversion.

References

[1] Pena MA, Gomez JP, Fierro JLG. New catalytic routes for syngas and hydrogen production. Applied Catalysis A 1996;144;7-57.

[2] Furimsky E. Selection of catalysts and reactors for hydroprocessing. Applied Catalysis A 1998;171;177-206.

[3] Rostrup-Nielsen JR. In J. R. Anderson & M. Boudart (Eds.), Catalysis, science and technology, Catalytic steam reforming vol. 5, Berlin: Springer, 1984.

[4] W He. Dynamic performance of a reformer for molten carbonate fuel cell power-generation systems. Fuel Processing Technology 1997;53;99-113.

[5] James L, Dicks A. Fuel Cell Systems Explained. Wiley, 2nd Ed., 2003.

[6] Xu J, Fromment GF. Methane steam reforming, methanation and water-gas shift. I. Intrinsic kinetics. A.I.Ch.E. J. 1989;35(1); 88-96.

[7] Boor CD. A Practical Guide to Splines. Springer-Verlag, New-York, 1978.